ISBN: 978-628-96613-3-0. ISSN: 2414-6390. Digital Object Identifier: https://dx.doi.org/10.18687/LACCEI2026.1.1.2777

The Design of an Autonomous VTOL Fixed-Wing Aircraft for Delivering Medical Supplies

Ryan Kurkela[1], Zaheer Haniff[2], and Ajward Wahid[3]
Faculty Mentor: Amir Elzawawy, P.H.D[1], Shouling He, P.H.D[2], and Alaric Hyland
[1]Vaughn College of Aeronautics and Technology, U.S., *ryan.kurkela@vaughn.edu*, ajward.wahid@vaughn.edu, amir.elzawawy@vaughn.edu
[2] Vaughn College of Aeronautics and Technology, U.S., *zaheer.haniff@vaughn.edu*, *shouling.he@vaughn.edu*, alaric.hyland@vaughn.edu

ABSTRACT

This project presents the design of an autonomous vertical takeoff and landing (VTOL) drone for delivering medical supplies to remote and underserved regions. The system uses a hybrid fixed-wing quadcopter configuration with tilting rotors, enabling efficient vertical takeoff and long-range fixed-wing flight. The drone transitions between flight modes by rotating its propellers. The design incorporates a tandem tilt-motor design to improve aerodynamic efficiency by reducing energy drain and propeller interference. Overall, the system provides a flexible autonomous medical delivery system.

I. INTRODUCTION

Access to medical supplies in remote regions remains a global challenge, often limited by terrain, infrastructure, and response time. This project addresses the gap through design and development of an autonomous vertical takeoff and landing (VTOL) drone capable of delivering medical payloads efficiently and reliably. By combining the advantages of VTOL and fixed-wing capabilities, the system is engineered to operate without the need of a launch system or certain landing locations, while still achieving long-range and efficient flight.

A. *Need and Objective*

This project focuses on developing an autonomous VTOL drone designed to deliver medical supplies to remote and difficult to access areas. The drone is capable of vertical takeoff and landing, then transitions into fixed-wing flight by tilting its propellers from a vertical to a horizontal position. It can autonomously navigate to designed locations and deploy supplies with precision. Powered by electric motors and advanced navigation systems, the design provides a cost-effective and environmentally friendly solution for transporting critical healthcare resources. Overall, it aims to improve accessibility, reduce delivery times, and better support underserved communities.

The objective of this project is to develop an autonomous drone capable of delivering medical supplies to remote areas with limited access to healthcare resources. The drone will be designed as a fixed-wing quadcopter that performs vertical takeoff and landing (VTOL). After takeoff, the propellers will tilt to transition the aircraft into fixed-wing flight for efficient long-distance travel.

Upon reaching the target location, the drone will switch to VTOL mode to land at the designated drop zone. Once positioned, a released mechanism will open to deploy the medical supplies and then securely close after the payload has been delivered. The drone will then take off again in VTOL mode, transition back to fixed wing flight, and return to its original launch location.

B. *Research and Impacts*

1)Background Research: This project builds on proven drone technologies, emphasizing safety, reliability, and autonomous operation. Like zipline platforms, it combines efficient flight with advanced sensing and navigation as shown in Figure 1 [7]. Unlike their launch-based systems, this design uses a tandem tilting- motor VTOL configuration, enabling VTOL and efficient fixed-wing flight while reducing aerodynamics interference and power consumption [1] .

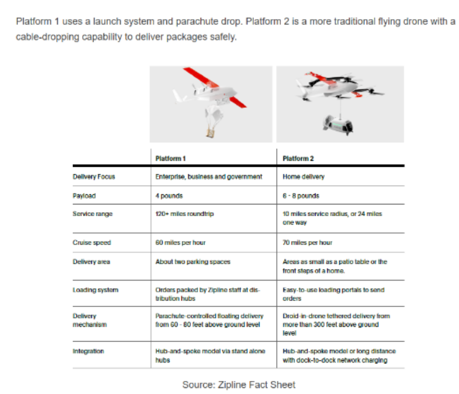
Platform 1 uses a launch system and parachute drop. Platform 2 is a more traditional flying drone with a cable-dropping capability to deliver packages safely.

	Platform 1	Platform 2
Delivery Focus	Enterprise, business and government	Home delivery
Payload	4 pounds	6 - 8 pounds
Service range	120+ miles roundtrip	10 miles service radius, or 24 miles one way
Cruise speed	60 miles per hour	70 miles per hour
Delivery area	About two parking spaces	Areas as small as a patio table or the front steps of a home.
Loading system	Orders packed by Zipline staff at distribution hubs	Easy-to-use loading portals to send orders
Delivery mechanism	Parachute-controlled floating delivery from 60 - 80 feet above ground level	Droid-in-drone tethered delivery from more than 300 feet above ground level
Integration	Hub-and-spoke model via stand alone hubs	Hub-and-spoke model or long distance with dock-to-dock network charging

Source: Zipline Fact Sheet

Figure 1: Zipline Platform 1 and 2 comparisons

2) Social Impacts: The system improves access to medical supplies in remote areas through fast, autonomous delivery. Applications in countries like Rwanda and India demonstrate how drones enhance healthcare and agriculture, highlighting their societal benefits [2].

3)Economic Impacts: Drone Delivery can reduce transportation costs by replacing traditional ways with efficient electric systems. Looking at the global drone market growing rapidly, this technology also supports industry expansion and job creation [3] and [5].

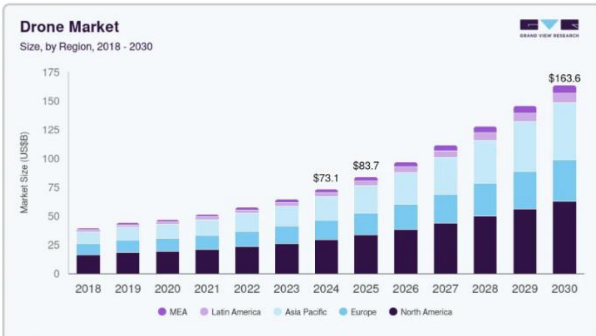

Figure 2: Chart showing the drone market increase from 2018 to 2030 [3]

The implementation of this autonomous drone delivery system has the potential to significantly reduce transportation costs within the medical supply chain. By replacing traditional delivery methods such as ground vehicles or large cargo aircraft with drones powered by electric motors, overall operating expenses can be lowered. The global drone market was valued at approximately $73.06 billion in 2024 and is projected to reach $163.60 billion by 2030, growing at an annual rate of 14.3% from 2025 to 2030. This expansion is driven by rapid autonomous systems, and enhanced imaging sensors, all of which continued to broaden drone applications across various industries.

4)Environmental Impacts: Electric drones lower carbon emissions compared to fuel powered transport and support environmental monitoring. Additionally, faster medical deliveries improve healthcare outcomes and emergency response, promoting global healthcare [4].

II. Electrical Components

Figure 3: E-Calc

For our E-Calc we received the results above with the component set up we used. We were able to receive a thrust weight of 2.6 when normally the goal is 2 and we have an anticipated flight time of 14 minutes. To increase that time, we would just need to buy a bigger battery that has a higher mAH rating. The main issue was temperatures since they were in the red, meaning the ESC's and motors are going to heat up a lot. But to counteract this, we used PETG and Poly carbonate in our manufacturing process due to their high thermal properties, ensuring nothing will be damaged.

A. Flight Controller (FC)

Figure 4: Cube Pilot the Cube Orange FD Standard Set + ADS-B

IO Ports: 14 PWM servo outputs

- 5X UART
- 2x can Ports
- I2C
- Input Voltage: 4.1v-5.7v
- Rated input current: 2.5A
- Rated input/output power: 14W
- 3 IMU's (Accelerometer/gyroscope)
- Dual barometers

B. Electronic Speed Controller (ESC)

Figure 5: SEQURE 100A Brushless Motor ESC 5-12S for RC Drones

- Dual-way brushless esc support 5-12 LiPo.
- Input Voltage 18V-50.4V, Continuous Current 100A, Peak Current 180A
- Support more protocols like Dshot (All), PWM, Oneshot, Multishot, etc.
- Functions: Forward, reverse, braking
- Low voltage protection, temperature protection, locked rotor protection, and current protection.
- Supports motor timing, throttle calibration, current detection, motor steering, telemetry signal and other settings.

C. *Motors*

Figure 6: P60 Pin Agricultural UAV Motor KV170

This motor was selected due to its optimal thrust-to-efficiency ratio, delivering maximum propulsive force while maintaining superior energy consumption characteristics. Through comparative analysis of available propulsion systems, this unit demonstrated the most favorable performance profile for our operational requirements. The motor's ability to generate substantial thrust without imposing excessive energy demands ensures extended flight duration and enhanced payload capacity, making it the most suitable choice for this application.

III. Wing Design and Aerodynamic Analysis

The development of the wing went through an iterative design and analysis process, prioritizing a high lift to drag ratio while maintaining a structurally sound wing that includes enough of a weight reduction to maximize the drone's medical payload capacity.

A. Wing Airfoil Selection

The aerodynamic performance of the NACA 4412 airfoil wing was analyzed using an XFLR5 software package [6]. The NACA 4412 was selected for its peak and sufficient lift to drag ratio values, specifically operating on the angle of attack values of –3° to 3°. When compared to competitor airfoils like NACA 2415, 4412 provides a more stable and progressive set of lift coefficient values and a set of pitching moment coefficient values closer to zero which in turn helps with overall stability and effectively reducing the workload on the flight control system. Further analysis and calculations led to the confirmation that the minimum velocity required for the horizontal flight portion of the flight remained below the 60-mph target within the angle of attack range, helping ensure that the drone achieves proper flight after catching enough speed via the VTOL portion. The values extrapolated via the XFLR5 wing analysis include the geometries for the wing airfoil, given NACA 4412 as the airfoil, and the geometries for vertical stabilizer, which ended up being the NACA airfoil 0012.

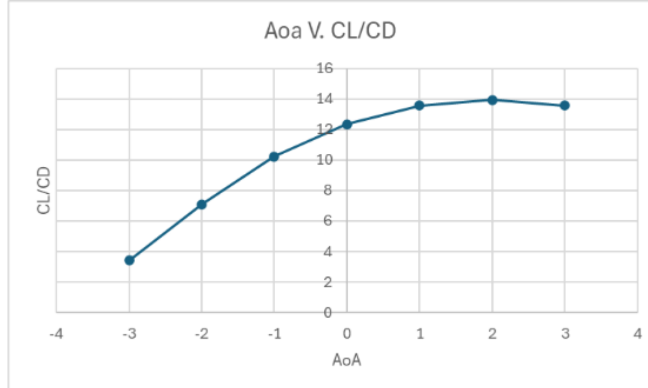

Figure 3: 4412 AoA v L/D

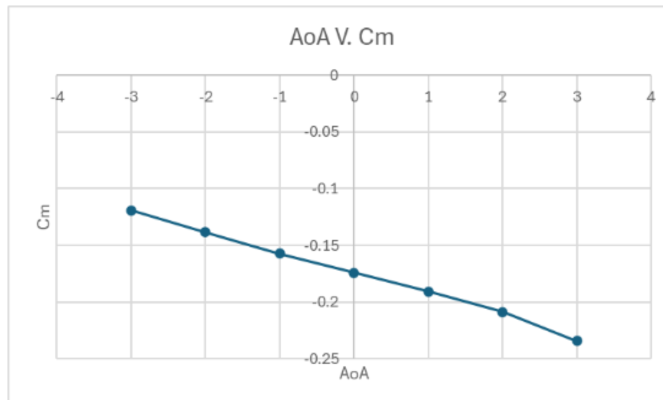

Figure 4: 4412 AoA v Cm

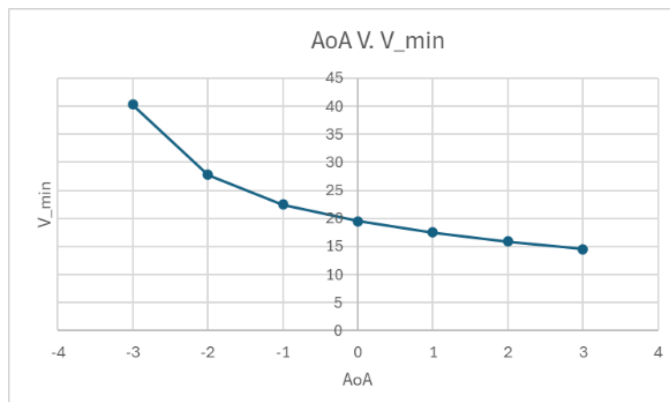

Figure 5: 4412 AoA v Vmin

alpha	Beta	CL	CDi	CDv	CD	CY	Cl	Cm	Cn	Cni	QInf	XCP	CL/CD	V_min
-3	0	0.066059	0.000384	0.018987	0.019371	0	0	-0.11919	0	0	11.176	-2.3313	3.410201	40.27136
-2	0	0.139015	0.001727	0.017837	0.019563	0	0	-0.13823	0	0	11.176	-1.0399	7.106016	27.76077
-1	0	0.212247	0.00405	0.016679	0.020729	0	0	-0.1574	0	0	11.176	0.0985	10.23913	22.46682
0	0	0.280793	0.007114	0.015617	0.022731	0	0	-0.17403	0	0	11.176	0.1253	12.35287	19.53301
1	0	0.350741	0.011125	0.014733	0.025858	0	0	-0.19076	0	0	11.176	0.1091	13.56412	17.47709
2	0	0.424494	0.016311	0.014112	0.030423	0	0	-0.20888	0	0	11.176	0.0976	13.95306	15.88644
3	0	0.507728	0.023312	0.014095	0.037407	0	0	-0.23422	0	0	11.176	0.0913	13.57307	14.52602
4	0	0.584484	0.030918	0.014276	0.045194	0	0	-0.25624	0	0	11.176	0.0861	12.93278	13.53867
5	0	0.6473	0.038009	0.014669	0.052678	0	0	-0.27041	0	0	11.176	0.0816	12.28786	12.86499
6	0	0.710482	0.04585	0.015192	0.061042	0	0	-0.28481	0	0	11.176	0.078	11.63923	12.27964
7	0	0.774173	0.054476	0.015781	0.070257	0	0	-0.29949	0	0	11.176	0.0751	11.01916	11.76368
8	0	0.838283	0.063905	0.01643	0.080335	0	0	-0.31442	0	0	11.176	0.0725	10.43484	11.30491
9	0	0.902295	0.074055	0.017146	0.091201	0	0	-0.32934	0	0	11.176	0.0703	9.893477	10.89653
10	0	0.96612	0.084926	0.01792	0.102847	0	0	-0.34422	0	0	11.176	0.0684	9.39376	10.53045

Figure 6: NACA4412 XFLR5 Analysis

B. Vertical Stabilizer Airfoil

The vertical stabilizer went through the engineering stages of analysis and design to provide the necessary directional stability for the drone, specifically to counter the asymmetrical thrust and yaw moments during the fixed wing stage of the drone.

The vertical stabilizer, although not physically manufactured and tested, needs to work uniformly to handle yaw in both directions, while the main wing serves its purpose as a tool that helps the drone achieve or create lift. For the vertical stabilizer, the specific air foil used was NACA 0012, and its selection was made because of two main reasons. The first reason was that NACA 0012 is proven to be very good at flight stability, specifically for drones. The other reason was because of the close-to symmetrical shape of the air foil. It is very important for the vertical stabilizer to be symmetrical, as it ensures equal aerodynamic response to positive and negative yaw angles, thus leading to stable directional control during fixed forward flight.

C. Horizontal Stabilizer Design

Like previously stated, during the plane and wing analysis in XFLR5, the horizontal stabilizer was included in the analysis along with actual wing. The graphs displayed in the previous text display this data.

The Vertical Tail Volume Coefficient (V_v) was used to figure out the stabilizers actual size. For this specific drone, a V_v of 0.55 was selected. Using this value, along with the drone's wingspan value and wing area value, the total area, height, root chord, and tip chord of the vertical stabilizer were found.

D. Tail Boom Specification

The vertical stabilizer will be held by a structural rod that would be extended from the rear of the drone. The length of this rod will help define the Tail Moment Arm, serving as the distance from the aircrafts center of gravity to the stabilizers aerodynamic center. The calculation of this Rod length uses the tail moment arm value and the root chord value, leading to a tail rod length value of 77.6 cm.

E. Structural Optimization

The overall structural design of the drone did go through an iterative design process, all in hopes of reducing the drone's total weight and improving manufacturing efficiency. When it comes to the wings internal structure, specifically the airfoil ribs, the thickness of each rib was cut down from 5 mm to 3 mm, as it was believed that the 2 mm extra thickness didn't serve any purpose besides adding weight. Also, specific square and hole cuts were changed from the cuts size and distance between each cut to keep up with design changes pertaining to the structural rods and fuselage design changes.

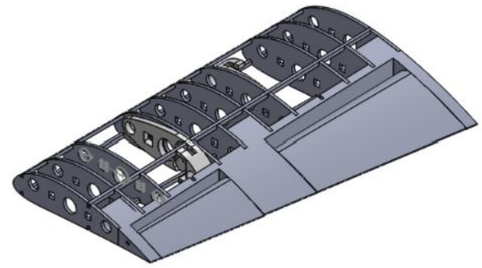

Figure 7: Full Wing Assembly

F. Flap Modification

The design of the flaps, too, went under design changes to optimize the wing, more specifically to help reduce drag and improve structural integrity. The flap connector, a piece created to hold the airfoil ribs and wing flaps, went through a design change where a three squared extrusion with a hole cut through all of them was added. This was to allow the connector piece to grasp the inner structural rod, creating a more robust mechanical connection. Another change was to the flaps, as they were extruded while having added a curved inner portion to reduce gap between the flap and the connector, thus reducing overall potential pressure silage during flight, leading to less drag.

G. Governing Equations

Taper Ration

$$\frac{TipChordLength}{RootChordLength}$$

Mean Aerodynamic Chord

$$\frac{\left(1 + TaperRatio(TaperRatio\ \cdot\ TaperRatio)\right)}{1 + TaperRatio}$$

Final Mean Aerodynamic Chord

$$\frac{2}{3} \cdot RootChord \cdot MeanAverageChord$$

Reynolds Number

$$\frac{1.225\frac{kg}{m^3} \cdot 17.9\frac{m}{s} \cdot FinalMeanAverageChord}{.0000181\frac{kg}{m \cdot s}}$$

Area Of Wing

$$WingSpan \cdot AverageChord$$

Coefficient of Lift Over Coefficient of Drag

$$\frac{CoefficientOfLift}{CoefficientOfDrag}$$

Minimum Velocity Required for Lift

$$\frac{\sqrt{2 \cdot Weight}}{1.225\frac{kg}{m^3} \cdot (C_L\ at\ AoA) \cdot AreaOfWing}$$

Reynolds Number Variables							
Density (kg/m^3)	Velocity (M/S)	Tip Chord length (m)	Root Chord (m)	Taper Ratio (m)	MAC (m)	Final MAC (m)	Dynamic viscosity (kg/(m*s))
1.225	11.176	0.17	0.225	0.755555556	1.325175809	0.198776371	0.0000181
Reynolds Number							
150351.8115							
Area of Wing Variables							
Wingspan (m)	Average Chord (m)		Length of One Wing (m)				
0.7	0.1975		0.35				
Area of Wing (m)							
0.13825							

Figure 8: Wing Design Calculations

H. Flap Control

All the flaps and ailerons were controlled by 180 degree turning servo motors. These servo motors were screwed into place, specifically into the servo motor holders, which were designed via SolidWorks and later 3D printed. They can be seen in Figure 7, specifically between ribs 3 and 4 as well as 7 and 8. Each wing requires two servos, as each servo controls one flap and one aileron.

In terms of wiring, each of the two servos wires for each wing were connected to one Y-Harness, then connected to a servo extension cable, in which the extension cable was connected to the FrSky X8R Receiver. This configuration allows for cleaner management of wires. In terms of operating the flaps and ailerons, a controller which communicates with the receiver helps with the tilting.

To connect the actual servo horns to the flaps, triangular pieces with 4 1mm hole cuts, aligned vertically to the long side of the triangle, were designed and 3D printed. They were then superglued to the flaps and serve as the other holding end. To connect the triangle piece to the horn, 1mm diameter push rods were ordered. Since only one side had the Z-shape, the other end of the rod had to be manually adjusted to make both sides have a similar Z-shape. This was done by clamping the rod to a bench vise and using a hammer and tweezer to create that needed Z-shape. Once completed, the push rods were inserted into one hole cut of the servo horn, and into one hole cut of the triangular piece.

IV. Fuselage Design

The aircraft features a structurally efficient fuselage and an integrated tilt-rotor system designed to balance strength, aerodynamic performance, and energy efficiency. The fuselage adopts a square cross-section with filleted edges, providing sufficient structural support for payloads and electronics while maintaining aerodynamic structure for long-range fixed wing flight as shown in Figure 9. This design prioritizes durability and stability, particularly during cruise conditions where efficiency is critical.

In the structure of the fuselage there are four sixteen-millimetre diameter rods that hold it together in the corners with four rib sections. It is squared shaped with filleted edges, the reason behind the shape is to allow for compartmentalization with placing electronics, the payload, tilt-rotor mechanism, and wings.

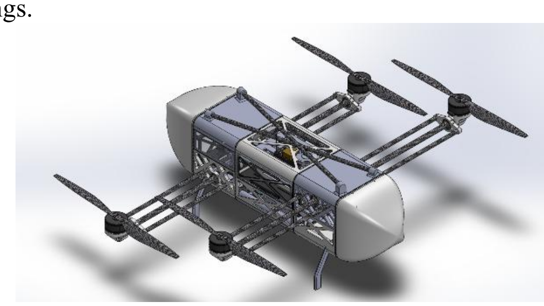

Figure 9: 3D Isometric View

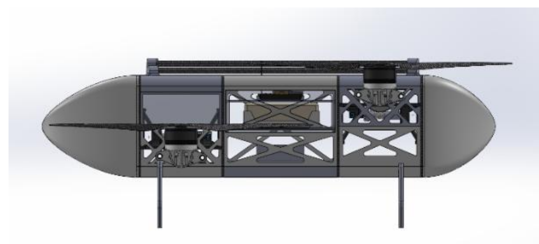

Figure 10: Side View

The overall configuration shown in Figure 9 draws inspiration from the tilt-rotor capabilities of the Bell Boeing V-22 Osprey and tandem rotor arrangement of the Boeing CH-47 Chinook. By combing these concepts, the design integrates a tandem tilt-rotor layout that enhances lift distribution and aerodynamic efficiency.

V. Programming and Configuration

Figure 11: Servo Settings

For our servo outputs we used the values 500-1900 for the 180-degree servos that were used for the drop mechanism and the flaps. Using these values allowed the servo to use its full distance of 0-180 degrees to allow the max amount of movement for the flaps and drop mechanism. The servos that are 1000-1900 are used for the 2 360 degrees servos to allow the full rotations and for it to stop at the midpoint of the tilt when the motors fully transition to 90 degrees and then allow the servos to rotate back up to the starting position of VTOL.

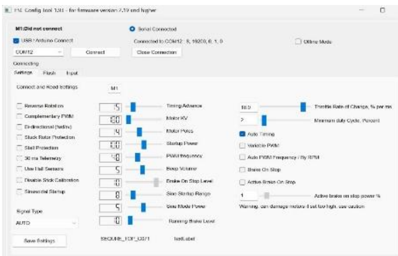

Figure 12: ESC settings

These were the ESC calibration set ups that were put into place with the default setting for the ESC to allow the motors to run at their max settings.

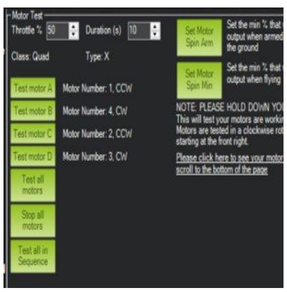

Figure 13: Motor Configuration

The orientation we have for the motors is the front right (Motor A) to be CCW, the back right motor (Motor B) to be CW, the back left motor (Motor C) to be CCW and the front left motor (Motor D) to be CW so that they are the same diagonally.

VI. Payload Drop Mechanism

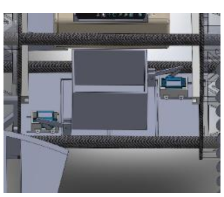

Figure 14: Closed doors

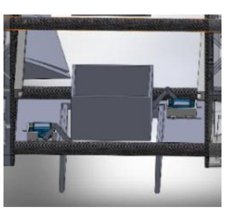

Figure 15: Open doors

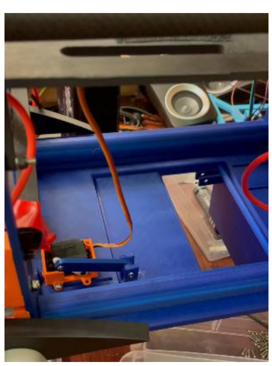

Figure 16: Tested

The payload drop mechanism is used to help deliver the medical supplies. This smooth transition consists of two 180-degree servo motors that move an arm attached to the door that swings open to allow the payload box to drop down as shown in Figure 14, 15, and 16. Throughout the duration of the flight, it keeps the doors closed and only opens the door during delivery. The payload is projected to weight no more than four pounds. The box is three feet by three feet square to allow for multiple types of supplies to be added inside.

VII. Tilt-Rotor Mechanism

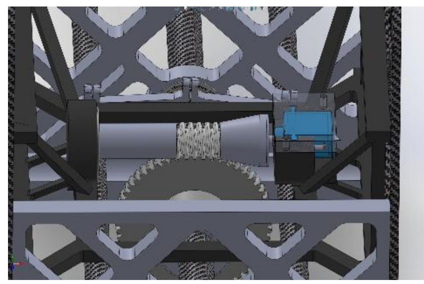

Figure 17: Front

Figure 18: Tested

The tilt-rotor mechanism is used on the front and rear rods as shown in Figure 17 and Figure 18, with the rear assembly mirroring the front. Each system utilizes a 360-degree metal servo motor connected to a circular horn, which drives a worm gear mechanism. As the worm gear rotates, it actuates a larger gear fixed to a perpendicular sixteen-millimetre diameter one-meter-long shaft that supports the motor mounts that hold the motors through a clamp on the rod, enabling controlled rotation of the propulsion system between vertical and horizontal positions. Calculations required for the tilt derive from the equations shown below being.

Loads:

Thrust from motor	$F = \frac{\text{max thrust}}{g} = \frac{8.5kgf}{9.8m/s^2}$ => **83N**
Motor weight	*W= (m) x (g) => (375g) x (*$9.81m/s^2$*) =>* **3.7N**
Apply Factor of Safety of 1.5-2 [8]	*Design Load = (F) x (FoS) => (83N) x (2) =>* **166N**
Total Force	*T = (Design Load) + (W) => (166N) + (3.7N) =>* **169.7N**
Moment from Rod	*L=0.5m, M=(T) x (L), M = (169.7N) x (0.5m) =>* **85N/m**

Moment of Inertia	$I = \frac{\pi}{64}(d_o^4 - d_i^4) => \frac{\pi}{64}(0.016^4 - 0.012^4)$ $=> \mathbf{2.2\ x\ 10^{-9} m^4}$
σ_b = Bending Stress c = Vertical distance away from neutral axis	$\sigma_b = \frac{Mc}{I} => \frac{(85\frac{N}{m})x\ (0.008m)}{2.2\ x\ 10^{-9}m^4}$ => 3.09 x 10^8 Pa => **309 MPA**

$\sigma_{allowable}$ FoS for Carbon Fiber that was used is 3	$\sigma_{allowable} = \frac{\sigma_{ultimate}}{FoS} => \frac{1000MPa}{3} =>$ **333MPa**
$\sigma_{allowable} vs\ \sigma_{actual}$	**333MPa > 309MPa**

FEA: For motor mounts

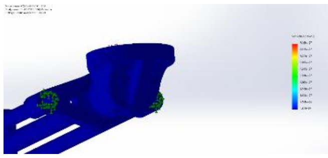

Figure 19: First FEA

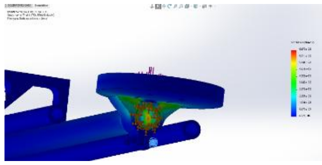

Figure 20: Final FEA

In SolidWorks, Finite Element Analysis was done for Figures 19 and 20 to see where the stress had occurred for the motor mount when the force will be applied. For aircrafts, a factor of safety of 1.5-2 was applied.

This mechanism enables smooth transition between VTOL and fixed-wing flight. As the rotors tilt forward, the wings begin to generate lift, reducing the load on the motors and lowering overall energy consumption. This improves flight efficiency, allowing for extended range or increased speed while minimizing power demand throughout the mission.

Figure 21: Picture of first hover test attempt

Figure 22: Picture of successful hover

VIII. Mission Objective

Overall weight	≤ 20lbs
Weight without payload	≤ 16lbs
Payload weight	≤ 4lbs
Wingspan	3.3ft
Speed	≤ 40mph
Distance travel	≤ 12+ miles one way
Electronics weight	≤ 3.7kg (8.6lbs)

VIIII. Discussion

Achieving a balance between efficiency and reliability is critical in the development of a fully autonomous medical delivery drone. This balance is reflected on the design, particularly in its hybrid flight capability. The drone can take off vertically and then transition into fixed-wing flight, enabling efficient long-range travel. Its ability to switch between VTOL and fixed-wing modes makes it especially effective in remote regions or areas with challenging terrain. The aircraft utilizes a tilt-rotor mechanism located at the end of its four wings. This tilting capability smooth transitions between vertical and forward flight modes. Additionally, the tandem rod placement and alignment improve motor efficiency during hover and transition phases.

The current draws inspiration from existing industry applications. Companies such as Zipline have demonstrated the importance of reliability and operational safety in autonomous delivery systems. As drone technology continues to advance, there is an increasing demand for improved autonomous applications. For instance, unlike Zipline's drones why rely on a catapult launch system, this design operates independently without the need for external launch equipment.

The significance of this project is further highlighted by its potential societal and economic impact. In countries like Rwanda, autonomous drones have already proven to be highly effective in delivering critical medical supplies, significantly improving emergency response times. The demand for reliable and efficient drone systems continues to grow, not only in healthcare but also in industries such as agriculture, and disaster relief. While this project mainly addresses healthcare, the application also makes it highly needed for other industries.

X. Conclusion

The development of an autonomous VTOL medical delivery drone represents a step towards improving access to essential healthcare in remote and underserved regions. By combining the vertical takeoff and landing capabilities of a quadcopter with the efficiency of fixed-wing flight, this design offers a practical and reliable solution for long-range, rapid delivery missions. Its innovative tilt-rotor mechanism and integrated structure enhanced performance during both hover and transition phases, while eliminating the need for external launch systems increases operational flexibility.

ACKNOWLEDGMENT

Advisors: Dr. Amir Elzawawy, Dr. Shouling He, and Alaric Hyland
Additive Manufacturing Assistance: Alaric Hyland
Test Flying: Michael Hefner
Engineering Department: Dr. Hossein Rahemi

REFERENCES

[1] Okulski, Michał. "A Small UAV Optimized for Efficient Long-Range and VTOL Missions: An Experimental Tandem-Wing Quad plane Drone." *MDPI*, 13 July 2022, https://www.mdpi.com/2076-3417/12/14/7059

[2] "Realizing societal benefits of drone tech through a pioneering airspace management system." *The World Economic Forum*, 29 May 2024, https://www.weforum.org/stories/2024/05/this-pioneering-airspace-management-system-can-unleash-the-societal-benefits-of-drone-tech/

[3] "Drone Market Size, Share & Growth | Industry Report, 2030." *Grand View Research*, https://www.grandviewresearch.com/industry-analysis/drone-market-report

[4] Wilcox, Joseph. "The Environmental Impact of Drones: What You Need to Know." *Flipswitch Films*, 24 April 2024, https://flipswitchfilms.co.uk/blog/the-environmental-impact-of-drones-what-you-need-to-know/.

[5] "3D-Printed Drones: Innovation and Advantages in Aerospace." *Weerg*, 24 January 2025, https://www.weerg.com/guides/3d-printed-drone

[6] A. Deperrois, "XFLR5": Analysis tool for airfoils, wings and planes operating at low to high Reynolds Numbers," version [V6.61], [2023]. https://www.xflr5.tech/xflr5.html

[7] "Zipline Safety Fact Sheet." *Zipline*, https://www.zipline.com/about/zipline-fact-sheet

[8] "Rigid High Strength Lightweight Carbon Fiber Round Tubes." *McMaster-Carr*, https://www.mcmaster.com/products/carbon-fiber-rods/rigid-high-strength-lightweight-carbon-fiber-round-tubes~~/od~5-8-2/od~0-625/carbon-fiber-construction~roll-wrapped/performance~high-strength-2/?s=carbon-fiber-rods

[9] "Carbon Fiber Tubes vs Steel: Weight, Strength & Cost Comparison 2025." *Income Pultrusion*, 2025, https://incomepultrusion.com/carbon-fiber-tubes-features-applications-and-manufacturing/

[10] Zobeiry, Navid. "Safety Factor, Building Block and Substantiation of Composite Aircraft." *Factor of Safety*, University of Washington, 11 06 2021, https://www.aidaa.it/wp-content/uploads/2021/06/10-11-June.pdf